

# Substorms observations during two geomagnetically active periods in March 2012 and March 2015

Veneta Guineva<sup>1</sup>, Irina Despirak<sup>2</sup>, Boris Kozelov<sup>2</sup>

<sup>1</sup> Space Research and Technology Institute, BAS, Stara Zagora, Bulgaria,

<sup>2</sup> Polar Geophysical Institute, Apatity, Murmansk region, Russia

e-mail: v\_guineva@yahoo.com

Accepted. 1 March 2016

**Abstract** In this work two events of strong geomagnetic activity were examined: the period 7-17 March 2012, which is one of the most disturbed periods during the ascending phase of Solar Cycle 24, and the severe geomagnetic storm on 17-20 March 2015. During the first period four consecutive magnetic storms occurred on 7, 9, 12, and 15 March. These storms were caused by Sheath, MC and HSS, and the detailed scenarios for the storms were different. The second event is a storm of fourth level with  $K_p = 8$ , the strongest one during the last four years, the so-called "St. Patrick's Day 2015 Event". A geomagnetic storm of such intensity was observed in September 2011.

Our analysis was based on the 10-s sampled IMAGE magnetometers data, the 1-min sampled OMNI solar wind and interplanetary magnetic field (IMF) data and observations of the Multiscale Aurora Imaging Network (MAIN) in Apatity. The particularities in the behaviours of substorms connected with different storms during these two interesting strongly disturbed periods are discussed.

© 2016 BBSCS RN SWS. All rights reserved

**Key words:** solar wind, storms, substorms, auroras

## Introduction

Events of strong geomagnetic activity are of special interest because magnetic storms can affect the energetic systems, the spacecrafts or the ground based systems. That's why coordinated actions of the scientific community are needed to perform and gather observations, to create models of the whole chain of phenomena from the Sun to the Earth in order to make successful predictions of space weather and to prevent failures in the technologic infrastructure due to strong geomagnetic storms (Schrijver et al., 2015). The present 24 solar cycle is distinguished by comparatively low solar activity. Up to now, in cycle 24, 14 geomagnetic storms with DST index less than -100 nT occurred (Watari et al., 2015).

It is known that the following types of solar wind mainly generate storms: ICME including Sheath region and body of ICME (magnetic cloud, MC) and CIR-region (e.g. Gonzalez et al., 1990). CIR (Corotating Interaction Region) is a region of the interaction of high-speed recurrent stream with undisturbed solar wind. CIR is determined as a region with magnetic field and plasma compression (Balogh et al., 1999). During a solar maximum, most common are the sporadic flows associated with coronal mass ejections (CME) (Webb and Howard, 1994). Near the Earth they are observed as magnetic clouds (MC) (e.g. Burlaga et al., 1982). The magnetic clouds (MC) are characterized as regions, where the magnetic field strength is higher than the average, the density is relatively low, and the magnetic pressure strongly exceeds the ion thermal pressure, the magnetic field direction changes through the cloud by rotating parallel to a plane which is highly inclined with respect to the ecliptic (Burlaga et al., 1982). Ahead of MC, a region of interaction with

undisturbed solar wind (Sheath) is known to form, which is characterized by high density, increased pressure and strong IMF variability. It should be noted that there are differences between storms generated by Sheath, MC and CIR (in intensity, recovery phase duration, etc.) (e.g., Huttunen et al., 2006; Pulkkinen et al., 2006; Yermolaev and Yermolaev, 2006).

However there are more complicated storm cases, when the magnetic storms are caused by several sources in the solar wind, coming consecutively one after the other or partly overlapping. Such cases, for example, are two events of strong geomagnetic activity: 7-17 March 2012 and 17-20 March 2015.

The first event on 7-17 March 2012 is one of the most disturbed periods during the ascending phase of Solar Cycle 24. This active interval was examined and the detected features were described (Tsurutani et al., 2014; Valchuk, 2013; Maris et al., 2014). During this period four consecutive magnetic storms occurred on 7, 9, 12, and 15 March, called S1, S2, S3 and S4, respectively. These storms were caused by Sheath, MC and HSS, and the detailed scenarios for the storms were different. Each individual storm was discussed in some detail in previous papers (Tsurutani et al., 2014; Valchuk, 2013).

The second event, on 17 March 2015, is the so-called "St. Patrick's Day 2015 Event". This is the principal event covering the interval from 15 to 18 March 2015, in which solar eruptive phenomena (a long-enduring C9-class solar flare and associated CME(s) on March 15 and a strong geomagnetic storm on March 17-18 (Max.  $D_{ST}$  was -235 nT) were reported. This magnetic storm is the largest one observed in the current solar cycle. A geomagnetic storm of such intensity was observed in September 2011.

In this paper aurora observations from Multiscale Aurora Imaging Network (MAIN) in Apatity connected with substorms during these two geomagnetically disturbed periods are presented. In the first event, 7-17 March 2012, we have measurements during three storm events, namely the first (S1), the second (S2) and the fourth (S4) storms of this period. Below one substorm event during the first storm (S1) - on 7 March 2012 is presented as an example. It should be noted that another event during the second storm (S2), 10 March 2012, has been described recently in our article (Guineva et al., 2015).

In the second disturbed period, 17-20 March 2015, we have measurements during the main phase of the geomagnetic storm, on March 17, 2015, and during the recovery phase of the storm, 18- 20 March 2015. Below two substorm events during the storm main phase, on 17 March 2015, and one substorm event during the recovery phase of the storm, on 20 March 2015 are presented.

## Data

Measurements from the Multiscale Aurora Imaging Network (MAIN) in Apatity during the strongly disturbed periods in March 2012 and in March 2015 have been used. The cameras observational system has been built in Apatity since 2008. It consists of 5 cameras with different fields of view providing simultaneous observations from two spatially separated points. The cameras characteristics, their mutual situation and the measurement process are described in detail by Kozelov et al. (2012). An all-sky camera and a Guppy F-044B (glass filter ~558 nm, field of view 18° diagonal) were installed on the main building of the Apatity division of the Polar Geophysical Institute, and another Guppy F-044B camera and a camera Guppy F-044C (field of view ~67° diagonal) were located in the Apatity range at a distance of 4120 m. All cameras were directed to a region near magnetic zenith. A special time synchronization module was developed. All cameras, data storage computers and motorized mounts are remotely accessible. One more camera Guppy F-044C, directed to North, was manually operated during good weather conditions.

To examine auroral phenomena usually both cameras images and keograms are used. A keogram represents a time versus zenith angle plot of the intensity created from the individual images. Therefore a pixel line in N-S direction (where North may be the geographic or magnetic one) is extracted from the consecutive images and the line values are drawn in vertical columns one after the other.

To study the substorm development data from the Apatity all-sky camera (images and keograms) and the Guppy F-044C (GC) camera with field of view ~67° (keograms) were used. The GC camera data were corrected regarding the exposition time, the gain, the heterogeneity of the dark field, and the objective transmittance change depending on the angle of observation. The keograms were constructed in

direction magnetic North (up). The zero angle coincides with zenith.

The solar wind and Interplanetary Magnetic Field (IMF) parameters were taken from 1-min sampled OMNI database ([http://sdaweb.gsfc.nasa.gov/cdaweb/istp\\_public/](http://sdaweb.gsfc.nasa.gov/cdaweb/istp_public/)).

Substorm presence was verified by the 10-s sampled IMAGE magnetometer data, namely the data of the meridional chain Tartu – Ny Ålesund (Tartu (TAR), CGM Lat.= 54.47° – Ny Ålesund (NAL), CGM Lat.= 75.25°).

## Observations

### *Interplanetary conditions during 7-17 March 2012*

The time interval 7 – 17 March 2012 (11 days) is one of the first major geomagnetically active periods of the ascending phase of SC24. Figure 1 presents the solar wind conditions taken from the OMNI database for the period 6-21 March 2012. In Figure 1 from top to bottom the Interplanetary Magnetic Field magnitude ( $B_r$ ), the IMF Z-component ( $B_z$ ), the flow velocity ( $V$ ), the X-component of the velocity ( $V_x$ ), the solar wind density ( $N$ ), the temperature ( $T$ ), the dynamic pressure ( $P$ ), the geomagnetic index AL, and the SYMN/H index are shown. Four geomagnetic storms developed during this time period, on 7, 9, 12, and 15 March, called the S1, S2, S3, and S4 events, respectively. In Figure 1 the onset times of these 4 storms are marked by vertical red solid lines and symbols S1, S2, S3, S4, respectively. It is seen that all storms were associated with high solar wind speeds and enhanced plasma densities and temperatures and interplanetary magnetic field strengths. These storms were caused by different sources in the solar wind (see details, Tsurutani et al., 2014; Valchuk, 2013). In this work we consider a substorm development during S1 storm. The S1 storm was caused by the southward directed Sheath fields (Tsurutani et al., 2014). The main phase of this storm started at ~ 02:00 UT on 7 March and reached a maximum at ~ 05:15 UT. The SYM-H peak intensity was ~ -100 nT.

Under these highly disturbed conditions, close to the SYM/H peak intensity of the S1 storm, in the near recovery phase, three substorms were observed at 18:45 UT, 19:39 UT and 20:15 UT, on 7 March 2012, by the all-sky camera in Apatity. The onset times of these substorms are marked by a blue vertical line. A second blue vertical line in Figure 1 marks the onset of the substorm on 10 March 2012, which observation was presented in the paper by Guineva et al. (2015). The first substorm on 7 March 2012 is presented as an example of substorm observations in Apatity during this highly disturbed period.

### *Substorm at 18:45 UT on 7 March 2012*

In Figure 2 the substorm development at 18:45:00 on 7 March 2012 is presented by measurements from the Multiscale Aurora Imaging Network (MAIN) in Apatity. The top panel shows selected images of the all-sky camera, and the bottom panel – the keograms by the all-sky camera (to the left) and by the Guppy (GC) camera (to the right). The world directions are

marked in the first image, the universal time is written above each image of the top panel.

The substorm was observed during the recovery phase of the S1 storm, near the maximal storm development. The value of SYM/H index at the moment of substorm onset was  $\sim -45$  nT. It should be noted that according to the observations of the chain of magnetic stations IMAGE, the magnetic disturbance began at Oulujärvi station (OUJ) at CGM Lat.= 60.99°N and moved to Sørøya station (SOR) at CGM Lat.= 67.34°N (the picture of the magnetic disturbances by IMAGE magnetometers is not presented here). As it is seen in Figure 2 substorm auroras appeared in the South part of the field of view at 18:45 UT. The auroras moved towards North, reached zenith at about 18:53 UT and after that auroras surpassed it. The substorm development can be studied in more detail by the GC keograms. In the GC keograms the substorm auroras are seen first at 18:52 UT. The maximal intensity of 120 rel. units was observed about 18:54:35 UT during the fast expansion to North. The substorm development is clearly expressed up to 19:10 UT.

### Interplanetary conditions during 17-20 March 2015

Figure 3 shows the solar wind conditions taken from the OMNI database for the period 16-27 March, 2015. Some solar wind and IMF parameters, the AL and SYM/H indices are presented. The format of Figure 3 is the same as the one of Figure 1. A severe geomagnetic storm (G4) developed during this time. It was the result of a pair of CME's that left the Sun on 15 March 2015, maybe unexpectedly combined when spreading towards Earth and formed a large shock front crossing the Earth orbit. At 4:45 UT a geomagnetic sudden impulse was registered in all stations of the IMAGE magnetometers network which indicated that the shock wave formed by the CME swept past our planet. It coincides with the storm sudden commencement when SYM/H index jumped from 16 to 66 nT. A Magnetic cloud passed the Earth and just after it a HSS superposed and contributed to the storm duration. SYM/H index reached the value -235 nT at 22:47 UT on 17 March 2015. The solar wind magnetic cloud (MC) and the high speed stream (HSS) regions are shown by shaded red (to the left) and green (to the right) rectangles, respectively, in Figure 3.

Under these highly disturbed conditions, 8 substorms were identified by the all-sky camera in Apatity: two of them occurred during the main storm phase, one – in the vicinity of the SYM/H peak, on 17 March 2015, five – in the recovery phase and in the late recovery phase of the storm, on 18 and 20 March 2015. Three examples of substorm observations are presented below - two substorm events during the storm main phase, at 17:36 UT and 19:59 UT on 17 March 2015, and one substorm event during the storm recovery phase, at 21:43 UT on 20 March 2015. The onset times of these substorms are marked by blue vertical lines in Figure 3.

### Substorm at 17:36 UT on 17 March 2015

In Figure 4 the development of the substorm at 17:36 on 17 March 2015 by measurements from MAIN in

Apatity is presented. The top panel shows selected images of the all-sky camera, and the bottom panel – the keograms by the all-sky camera and by the Guppy (GC) camera. The format of Figure 4 is the same as of Figure 2.

The substorm was observed during the main phase of the severe geomagnetic storm on 17 March 2015. The SYM/H value at the moment of substorm onset was  $\sim -163$  nT. Based on IMAGE magnetometers data, the magnetic disturbance began at Tartu (TAR) at 54.47°N CGM Lat. and moved to Ny Ålesund (NAL) at 75.25°N CGM Lat. (picture of the magnetic disturbances by IMAGE magnetometers not presented here).

As it is seen in Figure 4, substorm auroras appeared in the South part of the field of view at 17:36:40 UT. For some minutes auroras have stayed in the South part of the field of view. At 17:42 UT a fast motion towards North was observed and at 17:45:30 UT the auroras occupied the whole field of view. In the GC keogram, the substorm auroras are seen from 17:42:30 UT at the South part of the field of view, at 35° from zenith, due to the fast movement to North. Then a maximal intensity of 200 rel. units was observed about 17:46:25 UT.

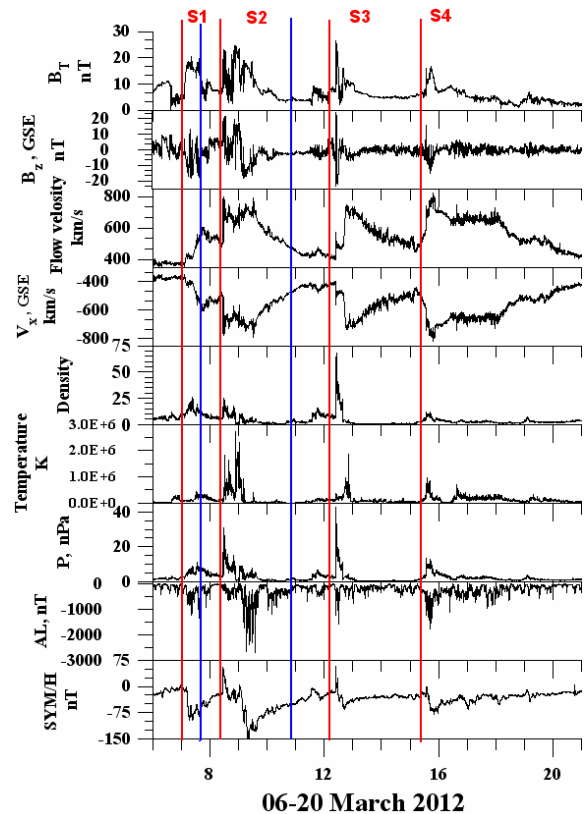


Figure 1 Solar wind and IMF parameters, AL and SYM/H indexes during March 6-21, 2012. Top-down: magnetic field magnitude, the IMF  $B_z$  component, the stream velocity  $V_x$ , the X component of the solar wind velocity, the density  $N$ , the temperature  $T$ , the solar wind dynamic pressure  $P$ , the geomagnetic index AL and the SYM/H index. The onset times of 4 storms are marked by vertical red solid lines and symbols S1, S2, S3, S4, respectively. The onsets of the substorms according IMAGE magnetometers network and all-sky camera in Apatity are marked by blue vertical lines.

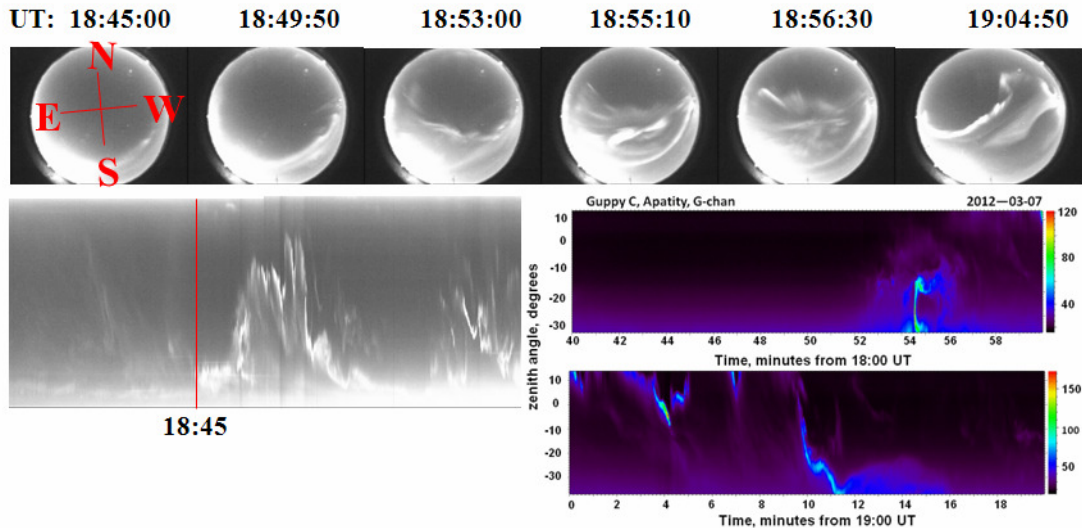


Figure 2 Development of the substorm in 18:45:00 UT on 7 March 2012 by chosen all-sky images (top panel), by all-sky keogram (left bottom panel) and Guppy (GC) camera keograms (right bottom panels). The world directions are marked in the first image, the universal time is written above each image

**Substorm at 19: 59 UT on 17 March 2015**

In Figure 5 the substorm development at 19:59 UT on 17 March 2015 is presented by selected images of the all-sky camera (the top panel) and keograms by the all-sky camera and by the Guppy (GC) camera (the bottom panel, to the left and right respectively). The format of Figure 5 is the same as of Figure 2.

This substorm was observed during the main phase of the severe geomagnetic storm on 17 March 2015. The SYM/H index at the moment of substorm onset was ~ -160nT. According to the observations of the IMAGE magnetometers, the magnetic disturbance as in the previous case (the substorm in 17:36 UT) began at Tartu (TAR) at 54.47°N CGM Lat. and moved to Ny Ålesund (NAL) at 75.25°N CGM Lat. (picture of the magnetic disturbances by IMAGE magnetometers not presented here).

The substorm by all-sky camera observations began at 19:59:40 UT. First auroras stayed to the South from the station zenith. At 20:24:30 UT a fast expansion to North was registered and auroras occupied the whole field of view. This time is marked in the all-sky keogram by a red vertical line. In the GC keogram the auroras at 19:59:40 UT are seen at about 25° to the South from zenith (the upper picture) and the rise at 20:24:30 UT is clearly expressed. The maximal relative intensity of the substorm auroras in the GC camera field of view was 70 rel. units. (60 rel. units at 20:36:40 UT at 15° to the North from zenith and 70 rel. units at 20:47:20 UT at 10° to the South from zenith, both during aurora flashes over the whole field of view).

**Substorm at 21: 43 UT on 20 March 2015**

In Figure 6 the development of the substorm at 21:43 UT on 20 March 2015 is shown by measurements from MAIN. Selected images of the all-sky camera (up) and keograms by the all-sky camera (bottom to the left) and by the Guppy (GC) camera (bottom to the

right) are presented. The format of Figure 6 is the same as of Figure 2.

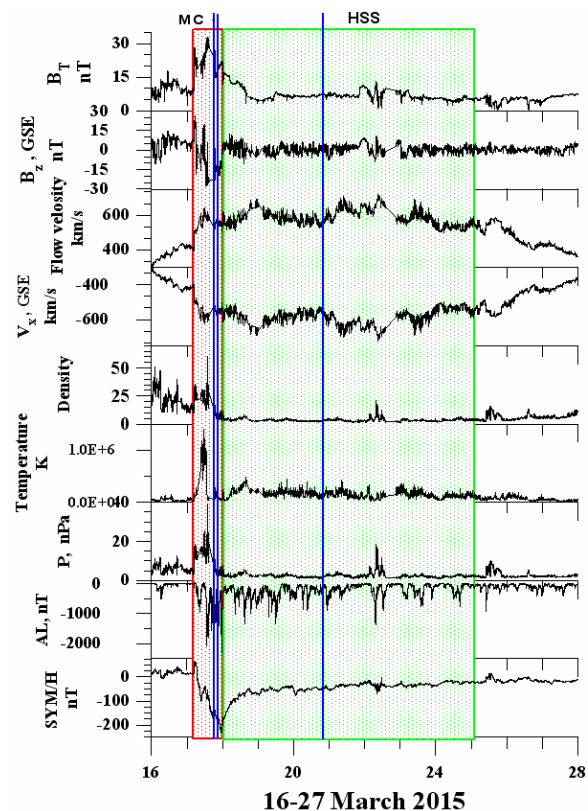


Figure 3 Solar wind and IMF parameters, AL and SYM/H indexes on March 16-27, 2015. The format of Figure 3 is the same as the one of Figure 1. The solar wind magnetic cloud (MC) and high speed stream (HSS) regions are shown by shaded red (to the left) and green (to the right) rectangles, respectively. The onsets of the examined substorms according IMAGE and the all-sky camera are marked by blue vertical lines.



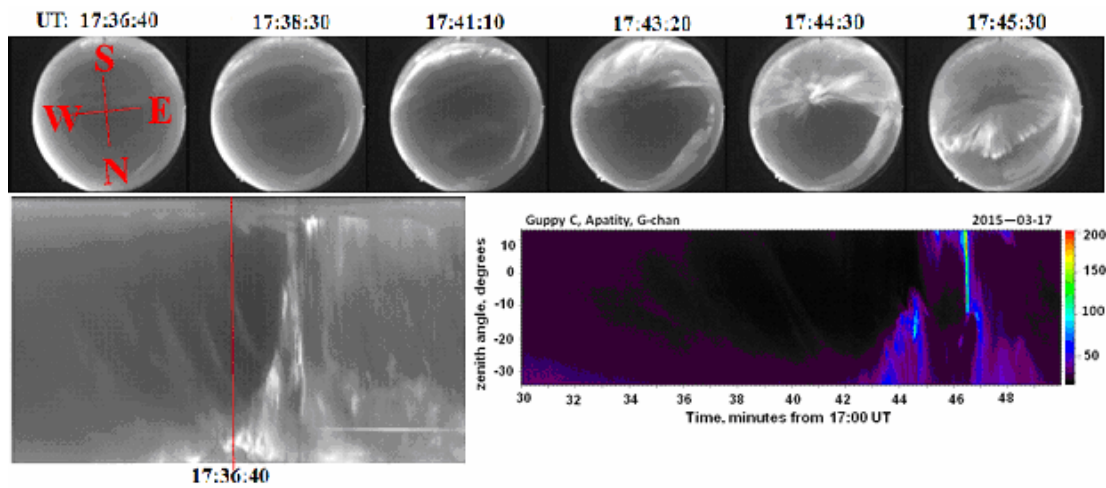


Figure 4 Development of the substorm in 17:36:40 UT on 17 March 2015 by chosen all-sky images (top panel), by all-sky keogram (left bottom panel) and Guppy (GC) camera keograms (right bottom panel). The format of Figure 4 is the same as the one of Figure 2.

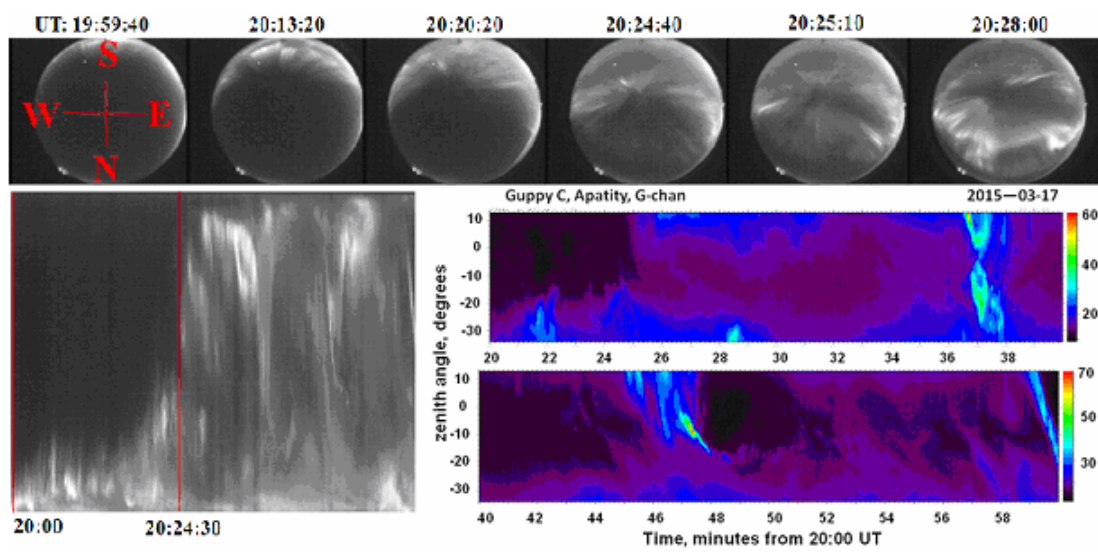


Figure 5 Development of the substorm in 19:59:40 UT on 17 March 2015 by chosen all-sky images (top panel), by all-sky keogram (left bottom panel) and Guppy (GC) camera keograms (right bottom panels). The format of Figure 5 is the same as the one of Figure 2

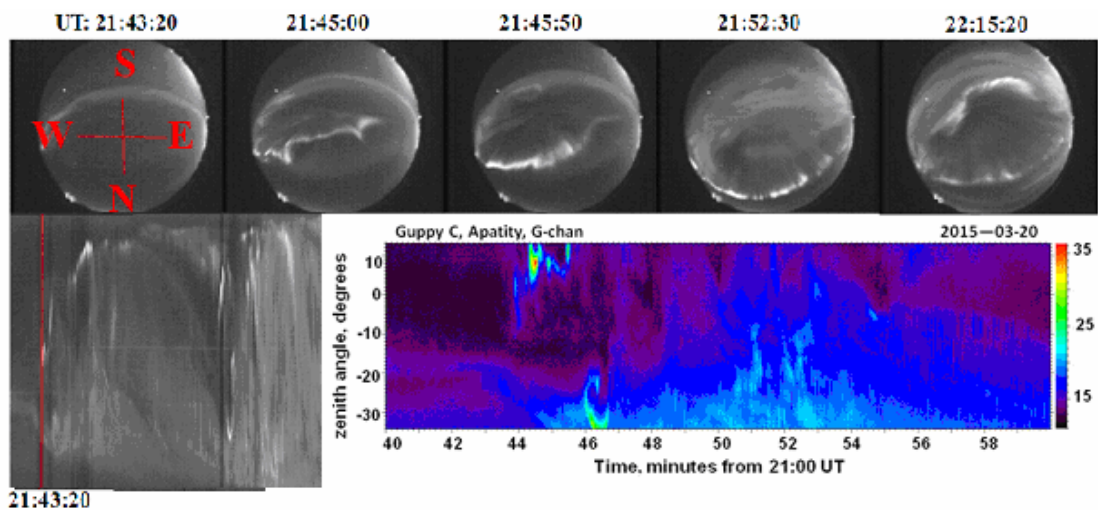


Figure 6 Development of the substorm on 20 March 2015 in 21:43:20 by chosen all-sky images (top panel), by all-sky keogram (left bottom panel) and Guppy (GC) camera keograms (right bottom panel). The format of Figure 6 is the same as the one of Figure 2

This substorm was observed during the late recovery phase of the severe geomagnetic storm on 17 March 2015. The SYM/H index value at the moment of the substorm onset was  $\sim -45$  nT. According to the observations of the IMAGE magnetometers, the magnetic disturbance began at Oulugärvi (OUJ) at  $60.99^\circ$  CGM Lat. and moved to Ny Ålesund (NAL) at  $75.25^\circ$  N CGM Lat. (picture of the magnetic disturbances by IMAGE magnetometers not presented here).

The substorm onset by all-sky camera observations was at 21:43:20 UT near the zenith of the Apatity station. The auroras expanded very fast, covered the whole field of view at about 22:16 UT and the station stayed inside the auroral bulge. In the GC keogram, the substorm onset is seen in the station zenith at 21:43:50 UT. The maximal intensity of 36 rel. units was observed about 21:44:30 UT during the auroras movement to North.

## Discussion

Storms are the final effect of the enhanced solar and interplanetary activity. So, it is important to have more observations of substorms during storms, especially under strongly disturbed conditions. We dispose of measurements from Multiscale Aurora Imaging Network (MAIN) in Apatity since 2009. During the period of MAIN functioning only 3 strong geomagnetic storms with  $D_{ST}$  less than  $-100$  nT occurred during the observational seasons and under clear sky conditions over Apatity – in March 2012, March 2013 and March 2015. In our work two of these three events of strong geomagnetic activity were examined, namely 7-17 March 2012 and 17-20 March 2015. We studied substorm events which were observed at different phases of these storm developments.

It should be noted that our observations confirm the movement of the auroras according to the dynamics of the auroral oval (see, for example, Starkov and Feldstein, 1971). In disturbed conditions, during the main phase of a geomagnetic storm or in the recovery phase close to the storm maximal development (the SYM/H peak value), the auroral oval is expanded, and substorm onset is to the South of the Apatity station, then the expansion of auroras to North can be observed. During the late recovery phase, when the auroral oval is "normal" or "compressed", substorm began to the North from Apatity, auroras moved from North to South in the field of view. These results confirm our previous studies (Guineva et al., 2015). The boundary between substorms generated to the South from the station latitude ( $63.86^\circ$  N CGM Lat.) and to the North from it in terms of SYM/H is in the range 40-50 nT and seems to depend on the level of the geomagnetic disturbance (which may be expressed by SYM/H peak value) and the distance in time from it of the substorm onset.

The maximal relative intensity in the camera field of view is greater for substorms arising to the South from the station and considerably smaller for substorm onsets in zenith or to the North from Apatity.

## Conclusions

It is shown that:

1. Substorms, originated during the main storm phase or near the SYM/H minimum in the recovery phase, occurred to the South of Apatity ( $63.86^\circ$  N CGM Lat.), and substorm auroras expanded in North direction.
2. For substorms during the recovery phase or the late recovery phase, auroras were observed near the station zenith or to the North of the Apatity station, and their motion from North to South was registered.
3. The boundary between both types of substorms in terms of SYM/H index is in the range 40-50 nT.
4. The maximal relative intensity of the substorm features in the camera field of view is considerably larger during the substorms arising to the South from Apatity.

## Acknowledgements

This study was supported by Program No 9 of the Presidium of RAS. The study is part of a joint Russian - Bulgarian Project 1.2.10 "The influence of solar activity and solar wind streams on the magnetospheric disturbances, particle precipitations and auroral emissions" of PGI RAS and IKIT-BAS under the Fundamental Space Research Program between RAS and BAS.

## References

- Balogh, A., Gosling, J.T., Jokipii, J.R., Kallenbach, R., Kunow, H.: 1999, *Space Sci. Rev.* 89, 141-411.
- Burlaga, L.F., Klein, L., Sheeley, N.R., Michels, Jr., Howard, D.J., Koomen, R.A., Schwenn, M.J. and Rosenbauer, H.: 1982, *Geophys. Res. Lett.* 9, 1317.
- Gonzalez, W.D., Gonzalez, A.L.C., Tsurutani, B.T.: 1990, *Planet. Space Sci.* 38, 181-187.
- Guineva, V., Despirak, I., Kozelov, B., 2015, *Sun and Geosphere* 10, 79-88.
- Huttunen, K.E.J., Koskinen, H.E.J., Karinen, A., Mursula, K.: 2006, *Geophys. Res. Lett.* 33, L06107, doi:10.1029/2005GL024894.
- Kozelov, B.V., Pilgaev, S.V., Borovkov, L.P., Yurov, V.E.: 2012, *Geosci. Instrum. Method. Data Syst.* 1, 1.
- Maris, M.G., Besliu-Ionescu, D., Georgieva, K., Kirov B.: 2014, 6<sup>th</sup> Workshop "Solar influences on the magnetosphere, ionosphere and atmosphere", 26-30 May 2014, Sunny Beach, Bulgaria, <http://ws-sozopol.stil.bas.bg/>.
- Pulkkinen, T.I., Ganushkina, N.Y., Tanskanen, E.I., et. Al.: 2006, *J. Geophys. Res.* 111, A11S17, doi:10.1029/2006JA011627.
- Schrijver, C.J. et al.: 2015, *Adv. Space Res.*, 55, 2745-2807.
- Starkov, G.V., Feldshtein, Ya.I.: 1971, *Geomag. and Aeron.* 11, 560.
- Tsurutani, B.T., Gonzalez, W.D., Gonzalez, A.L.C., Guarnieri, F.L., Gopalswamy, N., Grande, M., Kamide, Y., Kasahara, Y., Lu, G., Mann, I., McPherron, R., Soraas, F., V. Vasyliunas V.: 2006, *J. Geophys. Res.* 111, A07S01, doi:10.1029/2005JA011273.
- Tsurutani, B.T., Echer, E., Shibata, K., Verkhoglyadova, O.P., Mannucci, A.J., Gonzalez, W.D., Kozyra, J.U., Pätzold, M.: 2014, *J. Space Weather Space Clim.*, 4, A02, DOI: 10.1051/swsc/2013056.
- Valchuk, T.E.: 2013, *Astron. Tsirkulyar*, N1585, ISSN 0236-2457.
- Watari, S., Den, M., Kubo, Y.: Booklet of SCOSTEP-WDS Workshop on Global Data Activities for the study of Solar-Terrestrial Variability, 28-30 September 2015, [2-4], 22.
- Webb, D.F., Howard, R.A.: 1994, *J. Geophys. Res.* 99, 4201-4220.
- Yermolaev, Yu.I., Yermolaev, M.Yu.: 2006, *Adv. Space Res.* 37(6), 1175.